Carbon 206 (2023) 7–15

Contents lists available at ScienceDirect

Carbon

journal homepage: www.elsevier.com/locate/carbon

Effects of green solvents and surfactants on the characteristics of few-layer graphene produced by dual-frequency ultrasonic liquid phase exfoliation technique

Anastasia V. Tyurnina [a], Justin A. Morton [b], Amanpreet Kaur [b], Jiawei Mi [c], Nicole Grobert [d], Kyriakos Porfyrakis [e], Iakovos Tzanakis [b], Dmitry G. Eskin [a,f,*]

[a] Brunel Centre for Advanced Solidification Technology, Brunel University London, Kingston Lane, UB8 3PH, UK
[b] School of Engineering, Computing and Mathematics, Oxford Brookes University, College Cl, Wheatley, Oxford, OX33 1HX, UK
[c] Department of Engineering, University of Hull, Cottingham Rd, Hull, HU6 7RX, UK
[d] Department of Materials, University of Oxford, Parks Rd, Oxford, OX1 3PH, UK
[e] Faculty of Engineering and Science, University of Greenwich, Park Row, London, SE10 9LS, UK
[f] Tomsk State University, 36 Lenin. Ave, Tomsk, 634050, Russia

ARTICLE INFO

Keywords:
Graphene
Acoustic pressure
Ultrasonic exfoliation
Eco-friendly solution
Shock wave emission

ABSTRACT

Nowadays, one of the promising methods for scalable graphene production is ultrasound-aided liquid phase exfoliation (ULPE) of graphite. Two current limiting factors of ULPE are the use of harmful solutions (such as N-Methyl-2-pyrrolidone or Dimethylformamide) and a relatively low graphene yield. In this study, we demonstrate a new dual frequency (20 kHz and 1174 kHz) ULPE approach in various eco-friendly media, which enabled us to produce various few-layer graphene (FLG) solutions of high quality. By implementing sophisticated characterisation techniques consisting of Raman spectroscopy, UV–vis spectroscopy and high-resolution electron microscopy, the final graphene flakes structure was confirmed to correlate the properties of each individual solution. The thinner (~3 layers) and larger (~1.5 μm^2) flakes were observed while using just water, with the highest yield (11%) of smaller FLG flakes to be achieved in the mixture of water and a surfactant. In order to understand the cavitation mechanism in different solutions, the ULPE process was investigated by acoustic measurements. This study demonstrates the crucial role of ethanol (as a solvent) and surfactants as it regulates the cavitation power and intensity of the ultrasonic field and, thereby, the cavitation effectiveness. It is suggested that the mixture of water, ethanol and a surfactant is the best medium for ULPE process where a high yield of low-defective FLG flakes can be obtained in a solution stable at least for 3 months (around 80%).

1. Introduction

The ability to obtain a material in two-dimensional (2D) form, emerging from the isolation of graphene in 2004 [1], opened up the necessity for studying the 2D science phenomena and applying them in our daily lives. Mechanical exfoliation, allowing the separation of a single layer of graphite (SLG) or the so-called graphene, was the first top-down approach and still remains best in terms of obtained graphene characteristics: superior optoelectrical, quantum properties and superconductivity [2–4]. The drawbacks of the above-mentioned method include small size, high cost, extremely low yield and almost impossibility to scale up. Another top-down method widely popular today is the liquid phase exfoliation (LPE). It helps to overcome some of those challenges with much larger yield and scalability, although the produced few-layer graphene (FLG) flakes remain of even smaller size and concede the superior optoelectrical and quantum properties to those obtained by bottom-up approaches like chemical vapor deposition or epitaxial growth [5]. Nevertheless, interest into LPE is still growing nowadays due to its rather lower cost, higher yield, scalability, possibility to be eco-friendly and, finally, it does not require a complicated route of transferring the final graphene product to a substrate of choice [5]. In addition, the LPE produced graphene has significantly widened its application areas to biosensors/markers, conductive ink, water treatment, chemical, gas and air separators, seawater desalination, food processing, package engineering, CO_2 capture and storage to name but a few [6,7].

* Corresponding author. Brunel Centre for Advanced Solidification Technology, Brunel University London, Kingston Lane, UB8 3PH, UK.
E-mail address: Dmitry.Eskin@brunel.ac.uk (D.G. Eskin).

https://doi.org/10.1016/j.carbon.2023.01.062
Received 18 November 2022; Received in revised form 18 January 2023; Accepted 31 January 2023
Available online 3 February 2023

Currently, there are three main ways of performing liquid exfoliation to obtain graphene. The LPE can be performed via ultrasonication (US) (further called ULPE), shear mixing and by micro fluidization in pressurised microchannels. The last approach (developed a few years ago) is promising to be highly efficient with the recently reported graphene nanosheet yield of 100% [8–10]. Thickness of those sheets was not uniform (from 5 to 200 nm) and above 10 nm (dozens of layers (Ls)) on average, only 4% of the resulting flakes were <4 nm thick (could be considered as FLG [11]). However, the 100% yield of the process was reached by cycling the process (100 cycles, ~3 h). LPE by a shear mixer can provide more uniform and much thinner flakes (5–7 Ls), but of a smaller area (<0.5 mm^2) and with a very poor yield below 1% [9,12]. In recent years, ULPE where the cavitation bubbles play a crucial role in exfoliation under a controlled ultrasound field has attracted a lot of attention [13,14].

First of all, and foremost, any LPE method depends on the exfoliation medium [15]. There is a large volume of literature on the efficient exfoliation of graphite in N-Methyl-2-pyrrolidone (NMP) using different LPE approaches including shear mixer and microfluidization mentioned above. For the last decade the LPE users were challenged by the difficulties in removing harsh chemicals in the graphene production [16]. Green solvents and surfactants came into focus of LPE graphene manufacturers [9,17–19]. Water is not typically considered as an effective dispersant for exfoliation nor as a good stabiliser due to the mismatch in water and graphene Hansen solubility parameters [20], surface tension [21] and high graphite hydrophobicity [22]. However, there are several publications suggesting that the interaction between water and the graphitic surface had been underestimated [23–25]. Previously, we have also demonstrated the possibility of ULPE in pure water and have found out the key US parameters for the ULPE in terms of the final flake quality and yield [14,26,27]. The low and high frequency (Lf and Hf) ultrasound combination was one of the important conditions to obtain less defective FLG flakes of smaller thicknesses and larger sizes (3 Ls and 1 μm^2 on average, respectively). The dual frequency effect to ULPE of graphite was also explained in detail based on the acoustic analysis [26].

In order to further improve the yield and stability of as-produced FLG samples, in this paper we expand the use of the dual frequency ULPE to some basic green surfactants and solvents to reveal their effect on the final FLG characteristics. The impact of different green solutions to the final FLG flakes characteristics was analysed by means of Raman and UV–vis spectroscopies, and by high resolution transmission electron microscopy (HRTEM). Additionally, to understand the role of cavitation in graphite exfoliation, spectrum analysis was performed by *in-situ* measurements of acoustic emissions in a broad range of frequencies. Results revealed a promising combination of green solvents with surfactants that can significantly enhance the production of ULPE FLG and shift the paradigm from the use of harmful chemical solutions towards environmentally friendly solvents.

2. Methods and materials

As the initial source for graphene, commercially available graphite powder (GP) from Alfa Aesar was used. The average size of the initial GP particles was about 70 μm as per manufacturer's specification. Green chemicals such as ethanol (99.9% absolute grade) from Merck Life Science UK, dodecylbenzene sulfonic acid sodium salt (SDBS) and cholic acid sodium salt (SC) from Fisher Scientific were used as the eco-friendly [19] solvent and surfactants, respectively, mixed with pure deionized water (DIW) supplied by Lab Unlimited Carl Stuart group. The choice of the surfactants was based on the literature survey [18,20,28–31] and their concentration was adopted to our dual frequency ULPE process based on the yield measured after each exfoliation session.

The ULPE was performed in a dual frequency configuration as described elsewhere [26]. Briefly, a Lf 20-mm Ti sonotrode excited at 20 kHz was applied from the top of a beaker. A photo and a scheme of the set-up are shown in Supplementary Information, Fig. S1. The driving transducer (Sonic system, model L500/5–20) had 500 W power at 100%. It was immersed into the beaker center, 5-mm under the liquid surface. At the same time a Hf membrane transducer (Meinhardt Ultrasonics, multifrequency high power system E/805/T) made of a Ti diaphragm (50 mm in diameter, equal to the beaker diameter) created the US field from the beaker bottom at a working frequency of 1174 kHz (162 W for 50% power). The use of Ti tools can potentially add some Ti nanoparticles to the solution. This was tested in our previous work [26]and the amount of Ti nanoparticles was found to be negligible.

The ULPE procedure started with heating and degassing of the solvent in a 50-mm diameter clear PVC beaker (150 ml of DIW or a mixture of DIW and ethanol (WEt), 75 ml each [32]) by ultrasonicating it with the Lf sonotrode at 50% of input power for 15–20 min. The water or water-ethanol mixture temperature was stabilized at 50 °C for another 10 min. In the case of surfactant assisted ULPE, 15 mg of surfactant were added into the stabilized solvent (depending on the surfactant: in just DIW further names as WSC or WSDBC, in WEt – WEtSC) prior to GP. In all experiments, 60 mg of GP was added into the beaker and stirred gently by a Teflon spoon prior to US treatment. Both US sources were working at 50% of their maximum input power for 2 h at the stabilized temperature of around 50 °C (this temperature range is beneficial for ULPE as shown in Ref. [45]). To maintain the as-prepared mixture at the same temperature, a cooling arrangement was used around the beaker. The temperature was monitored by a K-type standard thermocouple with an RS 52 Digital Thermometer.

Based on the previous study of different possible regimes of US treatment [26] performed in DIW only, we have chosen to use the one when both sources worked simultaneously. The previous research showed that such a configuration provided the highest yield (9.7%), the lowest thickness (3 Ls) and relatively large final FLG flakes (1.5 μm^2). Results obtained earlier using the same settings but with a single, either Lf or Hf, source were used for comparison [14].

The as-prepared solution was divided straight after ULPE in 3 glass vials (50 ml each) and centrifugated (CF) at 1500 rcf for 30 min using a Sigma 2–7 Compact Benchtop Centrifuge. The upper part of the CF solution (about 30 ml) was immediately collected in cleaned glass vials in order to prepare several different supernatant samples for further advanced characterizations. Consequently, a drop of the CF solution was cast onto a precleaned Si/SiO_2 (300 nm) surface and dried at room temperature within a ducted fume cupboard prior to Raman investigation. Another 3 drops were put onto holey-carbon-coated copper grids (300 mesh) for HRTEM investigation and also dried at room temperature. Both dried samples were stored in plastic wafer-trays to be measured some days later.

UV–vis spectroscopy was carried out immediately after CF to prevent measuring the spectra when FLG flakes in the solution started agglomerating. A Hewlett Packard 8453 instrument was used to collect the spectra in the wavelength range 220–800 nm, which was enough to detect the graphene and potential graphene oxide related peaks expected at 270 [33] and 230 nm [34], respectively. For that, a certain amount of the CF solution was poured into a Cole-Palmer quartz cuvette (3.5 ml), with a path length of 10 mm, and measured with an acquisition time of 10 s.

An InVia Raman (Renishaw) spectroscopy system with Modu-Laser working at an excitation wave length of 514 nm was used to confirm the FLG structure, to verify the number of layers (NLs) by checking the 2D/G intensity ratios, presence of defects from the intensity ratios D/G and D/D′ (Fig. 1), and to trace the FLG structure quality after US process. The laser spot size was ~ 2 μm and the laser power was 0.2 mW. Raman spectra of 20–30 random flakes from each sample were registered in the range from 1200 to 3100 cm^{-1}. Data collection was made under 50 × magnification, the acquisition time was adjusted to have a reasonable signal/noise ratio.

A HRTEM 200-kV JEOL 2100 F Field Emission Gun was used to investigate individual FLG flakes in terms of their area and NLs. 30 to 45 representative flakes were investigated for each of the ULPE conditions.

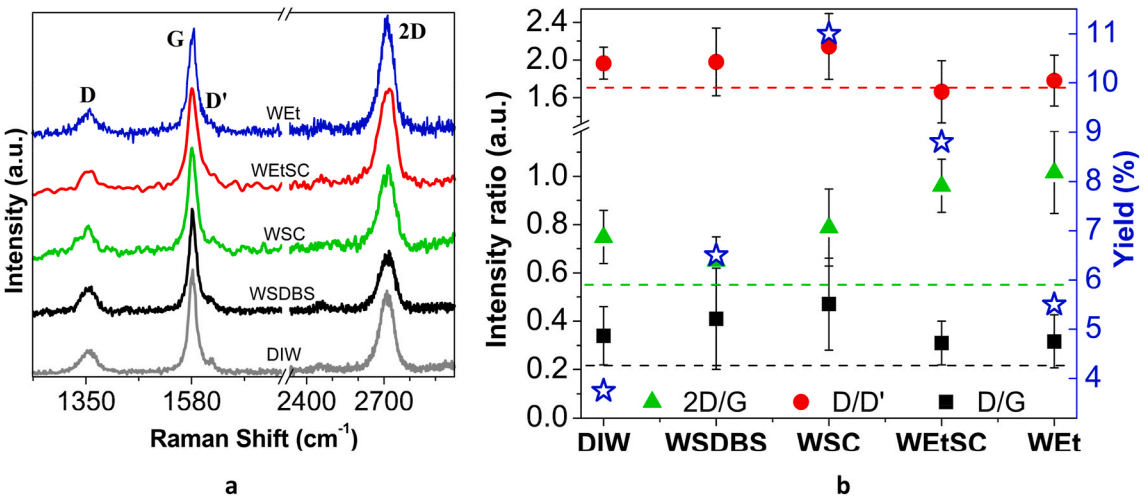

Fig. 1. Raman characterisation of as-produced FLG flakes samples. (a) Representative spectra from ULPE with different solutions; (b) average data of the Raman intensity ratios (left Y axis) for the Raman peaks shown in Fig. 1a (▲ - 2D/G; ● - D/D′ and ■ - D/G) for each of the ULPE produced sample of FLG flakes; these data for the original GP are shown by dashed lines of the same colour as the data for ratios. The data of the yield of the corresponding ULPE process are shown by blue open stars with numbers on the right Y axis. (A colour version of this figure can be viewed online.)

Further image processing was performed with ImageJ software in order to estimate the surface area and thickness of each flake. Statistical analysis of the measurements was performed.

After centrifugation, the top part of the solutions (about 100 ml) was vacuum filtered and dried in a vacuum overnight to determine the final concentration of the FLG flakes. The 0.2 μm pore PTFE membrane was used to collect the FLG flakes during filtration. The membrane was weighed prior and after filtration. The mass difference gave us the idea of final concentration of as-prepared FLG flakes and was used for yield estimation.

A calibrated (between 1 and 30 MHz, Precision Acoustics Ltd) fibre optic hydrophone was used to collect acoustic pressure measurements and acoustic spectra from ultrasonic cavitation clouds generated by the Lf sonotrode and Hf source transducer [35]. The sensor was positioned ~ 8 cm above the Hf source and ~ 2 cm below the sonotrode tip, in a location suitable for detecting high energy cavitation and shock waves (SWs) [35] that were previously identified as the prominent exfoliation mechanism during ULPE [27].

3. Results

3.1. Raman characterisation of all samples

As-prepared samples of the exfoliated GP were investigated by means of Raman spectroscopy to determine the structure of the flakes, to estimate their thickness and quality in terms of defects types and amount. All samples demonstrated the Raman spectra typical of sp^2 hybridized carbon materials. Fig. 1a contains the spectra examples of the FLG flakes samples produced in different studied solutions. For easier comparison all spectra were normalized to the intensity of the G peak around 1580 cm^{-1} related to the in-plane vibrational G mode. As it can be seen from Fig. 1, in addition to the G band of similar shape and full width at half maximum (FWHM) for all spectra, plots also demonstrate 3 additional defect related peaks at 1350, 1620 and 2700 cm^{-1} - so called D, D' and the second order of the Raman scattering 2D modes, correspondingly [36]. Among the studied spectra these bands are slightly varied in intensity but significantly differ in the average intensity ratios between the bands for different ULPE set-ups as shown in Fig. 1b. Those ratios are typically used to analyse the quality and the thickness of FLG flakes [37].

The number of defects is proportional to the value of D/G intensity ratio (black squares in Fig. 1b). As one can see the average value of D/G is the lowest for the spectra of the original GP (black dashed line). This ratio is doubled for the ULPE in DIW with surfactants (WSDBS and WSC cases). With the addition of ethanol, the ratio reduces to the level lower than the level of defects observed in DIW ULPE. Thus, adding the surfactants increases the number of defects, but adding the ethanol helps to reduce them. At the same time according to Refs. [13,38,39] D/D' intensity ratio (red circles for samples and red dashed line for GP in Fig. 1b) can be used to predict the type of those defects. For all the conditions used the average of that value was below 3.5, which is characteristic of the graphite edge-type defects rather than some planar disorders. Therefore, the apparent rising in the amount of defects happens likely due to the FLG flake size reduction to the dimensions smaller than the laser spot size diameter (2 μm) so that the edges contribute to the spectrum.

The other ratio 2D/G (green triangles in Fig. 1b) is commonly used for FLG flakes thickness estimation [13,38]. According to the data presented in Fig. 1b, the 2D/G intensity ratio increases compared to that of the original graphite source, which indicates the thickness reduction of the original GP (green dashed line). The highest average value of 2D/G intensity ratio (around 1) is registered for the samples obtained in the ULPE process in the WEtSC solution. Such a Raman characteristic is typical of FLG flakes with the thickness below 5 Ls [39]. Examples of some Raman spectra with characteristics corresponding to 1–2 Ls graphene are given in the Supplementary Information (Fig. S2) for each of the processes. The 2D peak shape analysis has shown that half of the 2D bands obey asymmetrical shape typical to Bernal stacking graphite [36]. Another half can be easily fitted with only one Lorentzian peak and the averaged FWHM of those is around 50 cm^{-1}, which can be a sign of turbostratic graphite [40]. Nevertheless, our detailed HRTEM investigation detected the layer spacing being in the range of 0.333–0.337 nm, while for turbostratic graphite its typical value would be 0.34 nm [41]. The observed 2D band widening is likely to be caused by flakes folding and overlapping with other flakes on the Si substrate during the drop casting and drying step.

The yield data (at the right Y axis in Fig. 1b) for each tested ULPE setting are shown by the open blue stars. Based on the correlation with the Raman characteristics, samples produced in WSC or WEtSC show effective exfoliation process with a yield higher than 8.5%. The WSC sample demonstrates the highest yield (11%) but also a higher defect level, while the WEtSC sample has significantly less defects at a slight expense of the yield.

3.2. TEM characterisation of all samples

To further understand the real thicknesses of the exfoliated material, a detailed investigation was performed by means of low and high-resolution TEM. One of the representative FLG flakes, obtained in the ULPE dual frequency set-up in the WSC solution, is shown at a low magnification in Fig. 2a, while the number of its layers (4 Ls) is shown in the high-resolution TEM image in the inset. The TEM results of all investigated flakes are summarized in Fig. 2b as an average data for the number of layers against the average area for all tested ULPE conditions.

The TEM data for DIW ULPE from the previous work [26] was used here for comparison, and is indicated by blue open star in Fig. 2b. The flakes produced in DIW using dual frequency ULPE were of a larger averaged size with the average thickness of 3Ls, but the yield of the process was very low (3.75%). Adding the ethanol or surfactant to the DIW helps to overcome this drawback. As it is shown in Fig. 1b the yield is rising up to 11% when SC is added to DIW. While the average thickness of the WSC flakes (4 Ls, red open star in Fig. 2b) is close to those obtained in just DIW ULPE (3 Ls, blue open star), the former are significantly smaller in size (average area is ~0.5 μm^2). When SDBS is mixed with DIW, the yield is almost doubled (6.5%) compared to the DIW sample (Fig. 1b), but also the average flake thickness doubles up and the flake area is reduced to 1 μm^2 (black open triangular in Fig. 2b). The addition of ethanol (to DIW) has the same effects on yield, size and thickness of the final FLG flakes, but the size is slightly larger (green circle in Fig. 2b) and the thickness is closer to 6Ls (on average). It is worth to note that ethanol also decreases the defects level as it has been already shown in the Raman results (Fig. 1b). This observation was also registered for Lf ULPE set-up and described elsewhere [42] as the consequence of the cavitation bubble size reduction, which led to gentler exfoliation. Interestingly, the dual frequency ULPE using the combination of ethanol and SC in DIW seems to be a good compromise between other studied ULPE settings. As one can see from Figs. 1b and 2b (grey open square), FLG flakes produced in WEtSC solution are thinner than those prepared in WEt, larger than those exfoliated in WSC and deliver a significantly higher yield, 3 times more compared to the yield in DIW exfoliation process; also demonstrating the lowest level of defects.

3.3. Stability of FLG in the studied solutions

Another important parameter of the as-produced samples of FLG flakes in different ULPE settings is the final suspension stability. Four of the described above samples were stored carefully for UV–vis characterisation at a later time. The UV–vis analysis was difficult in the case of SDBS surfactant as the SDBS related absorbance peak was wide and overlapped with the graphene related one [43], see also Supplementary Information Fig. S3. Additionally, the yield of the FLG flakes solution in the WSDBS medium was similar to the WEt sample and not as good as that in the WSC mixture. FLG flakes exfoliated in DIW are known to form a weakly stable solution [21,22]. In our ULPE experiment in DIW the flakes concentration dropped 50% after the 1st week of preparation. Its stability was monitored by the sample's UV–vis signal at 660 nm (Fig. 3a, black circles). Absorbance at this wavelength is proportional to flakes' concentration [44]. Then the UV–vis intensity of that sample mixture continuously reduced down to 1% after 2 more months and became almost zero one more month later. Addition of SC and ethanol can improve the stability (red squares and blue stars, respectively, in Fig. 3a). As one can see, after 50 days the concentration of the FLG flakes in both solutions stayed around 60% of the 1st day concentration measured right after CF. The WEt solution stabilized the FLG flakes concentration even above 70%, at least during the first 4 months (Fig. 3a, blue stars). Finally, the mixture of water/ethanol with the SC surfactant (Fig. 3a, open grey squares) increased the stabilized

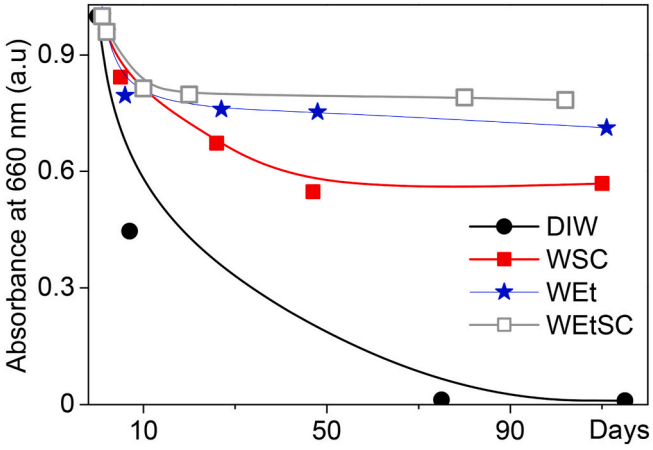

Fig. 3. Stability of the FLG flakes in different tested solutions. UV–vis absorbance at 660 nm vs days, normalized to the UV–vis absorbance measured on the day of the solution preparation. (A colour version of this figure can be viewed online.)

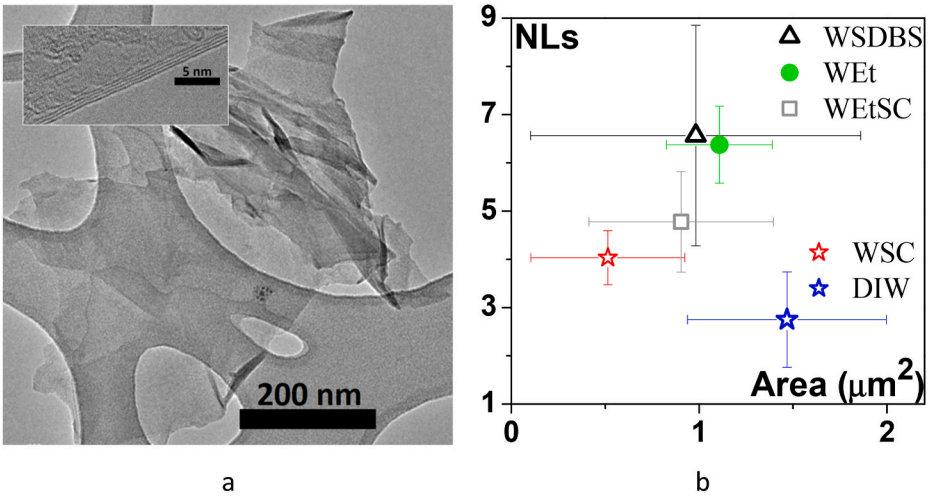

Fig. 2. TEM characterisation of as-produced FLG flakes: (a) TEM image at low and high resolutions (HR, inset) of a typical FLG flake obtained after ULPE process in the WSC solution; (b) the average data of the FLG flakes area and thickness obtained in different ULPE conditions. (A colour version of this figure can be viewed online.)

concentration up to almost 80% from the initial concentration. The exact percentage of concentration of the solution left after 4 months is shown in Table 1.

We can conclude that mixing ethanol and SC with DIW improved not only the ULPE yield and quality (lowest level of defects), but also the stabilisation of the FLG flakes concentration in the solution.

4. Discussion

4.1. Surfactant role in the exfoliation efficiency (yield)

Based on the TEM results presented in Fig. 2, one can conclude that the ULPE in DIW gives good results in terms of the small thickness (3Ls) and large area (1.5 μm^2) of as-produced FLG flakes. Unfortunately, the ULPE performed only in water is not effective from the viewpoints of both the yield, which is very low (about 3.75%), and the suspension stability (Fig. 3). A surfactant can promote the exfoliation process by assisting the dispersion in water or any other mildly volatile solvents [16,45]. The effect of surfactants has been well described in the literature. Coleman and Lotya were among the first to demonstrate in 2009 [20,28] the stabilisation effect of FLG flakes in water with added surfactants. Due to the effect of a surface charge, surfactants adsorbed by the graphite sheets produce Coulomb repulsion between them, acting against their reaggregation. It was noted that the surfactant concentration is a crucial factor for the stabilisation effect, but can be a limiting factor in some cases due to high concentrations required.

In order to improve the exfoliation efficiency in our unique dual frequency ULPE process 2 different eco-friendly surfactants were tested, SDBS and SC. As shown in Figs. 1–3 we have registered not only the stabilisation improvement and the number of defects' rising (rather due to the smaller flakes' size), but also a drastic increase of the yield. As we expected, both surfactants have improved the final concentration of the FLG flakes. Notley [46] has shown that the surfactants actually play a dual role. Firstly, being absorbed onto the exfoliated flakes surfactant molecules prevent their reaggregation, providing better solution stabilisation. Secondly, the liquid-vapor interfacial energy is lowered to the optimum level that is still enough to separate the sheets beyond the range of the van der Waals forces. While the stabilisation effect is rather clear and in accordance with the 1st role of the surfactant, the significant increase in exfoliation efficiency (yield) observed in our study could be explained by the combination of the optimum surfactant-induced interfacial energy and the specific pattern of US cavitation created by dual low and high frequency US fields. In our case the effect of the SC surfactant was much stronger for the yield than for the stabilisation. To the best of our knowledge, such a high yield of FLG flakes obtained in a WSC solution was not previously reported (except the cases where recirculation was involved [10]). We link that observation to the specific acoustic field created by the unique dual frequency set-up.

An additional acoustic investigation was carried out to clarify the influence of US parameters onto the dual-frequency ULPE efficiency in the solution with SC surfactant. As it was demonstrated before [26,27] the cavitation is the driving force for ULPE and can be characterised by acoustic emissions. In the current study, we measured acoustic spectra and pressure using acoustic sensors calibrated in a high-frequency range, capable of capturing the acoustic emissions associated with cavitation noise and shock waves (Section 2). Acoustic spectra of the four different solutions in the dual frequency configuration were measured (Fig. 4a and b) and the corresponding root-mean-square (RMS) acoustic pressures were then compared in Fig. 4c. The experimental procedure was described in detail elsewhere [26]. The four acoustic spectra in the range from 1 to 5 MHz, corresponding to four different tested solution mixtures (indicated in the legend of the figure by different colours) with their corresponding pressure-time profiles (shown by the inset waveforms) are presented in Fig. 4a.

DIW exhibits a more homogeneous waveform with less pressure fluctuations (this is typical of cavitation in water) though with multiple distinguished peaks (prominently emerged from the main waveform pattern) as indication of SWs. WSC solution follows a similar behaviour with prominent peaks visible on the waveform around the first 10 ms, though the pressure signal looks more chaotic with enhanced cavitation noise (up to 200 kPa). An extended cavitation zone with various cavitation clouds and myriads of vibrating bubbles produces pressure fluctuations over-imposed onto the incident frequencies as previously seen in Ref. [42]. The parts of the waveform that does not show prominent shock wave peaks (e.g. first 5 ms as well as towards the end after 15 ms) maybe indicative of blockage/shielding effects by the suspended clouds/bubbles diminishing SWs intensity as has been also reported in Ref. [47]. In the case of WEt the addition of ethanol forms a significantly wider pressure waveform (about 2 times larger in magnitude than in water, e.g. the section after 18 ms) indicating the development of an extended cavitation zone (with multiple emissions from a range of bubbly clouds). Prominent peaks apparent in the beginning become then hidden by the enlargement of the cavitation noise. This is expected as the formation of a bubbly mist can absorb shock waves intensity while expanding significantly the cavitation zone [42,48]. In the case of adding ethanol in the WSC the waveform also shows broadening of the cavitation noise due to more bubbles/clouds oscillations but also presents sharp peaks attesting for the SW propagating in the liquid solution. In general, after the cavitation becomes developed (as a function of the liquid properties), all tested liquids show the development of SWs with their intensity being a function of shielding by the bubbly clouds [49] and non-collapsing deflations [50].

It is also obvious that the solutions with ethanol demonstrate much more vigorous cavitation (broader white noise in the waveforms) but with lesser intensity of the generated SWs indicated by the rise of the hump in the range of 3.2–3.5 MHz (Fig. 4b) as has been previously explained in Ref. [35]. On the other hand, the sharp peaks observed in the same range for all the ethanol-based solutions, for example see prominent green line peaks in Fig. 4b, correspond to the harmonics of the incident wave (source of 1174 MHz) that are over-imposed by the vigorously vibrating water/ethanol bubbles with a resonance size of a few microns as also has been previously seen in Ref. [51]. Due to the Hf source, the 3rd harmonic also lies near this SW region and is likely to promote bubble oscillation at this frequency, lessening the effect of the SWs in ethanol-based solutions and perhaps promoting more uniform and gentle US exfoliation through smaller but vigorously oscillating cavitation bubbles. This could explain less defects of the as-obtained FLG flakes as compared to those of the samples from ULPE process in WSC medium. Thus, in the case of WEt solution we have a less aggressive cavitation regime occurring in a wider cavitation zone (as previously seen with the mist formation [42,48]), which promotes a gentler exfoliation in a larger area, in line with the results in Ref. [26]. This is also reflected by Fig. 4c where the RMS pressures (the mean square of the full waveform that represents the cavitation noise at the frequency range of 1–5 MHz) are higher for the ethanol- and SC-containing solutions. There is also a good correlation between the RMS data (Fig. 4c, left vertical axis) and the yield (right vertical axis – round symbols). In addition, it is interesting to note that the addition of SC in water forms a sharper hump compared to water alone, indicating a higher intensity of the propagating SWs. However, the more powerful the SWs, the less the quality of the flakes due to the induced defects. This is in a very good agreement with results in Figs. 1 and 2 where the exfoliation in WSC produces the

Table 1
The percentage of retained FLG flakes in DIW-based mixtures after 3+ months for different solvent compositions.

ULPE conditions	Percentage of the left material
DIW	1%
WSC	57%
WEt	71%
WEtSC	78%

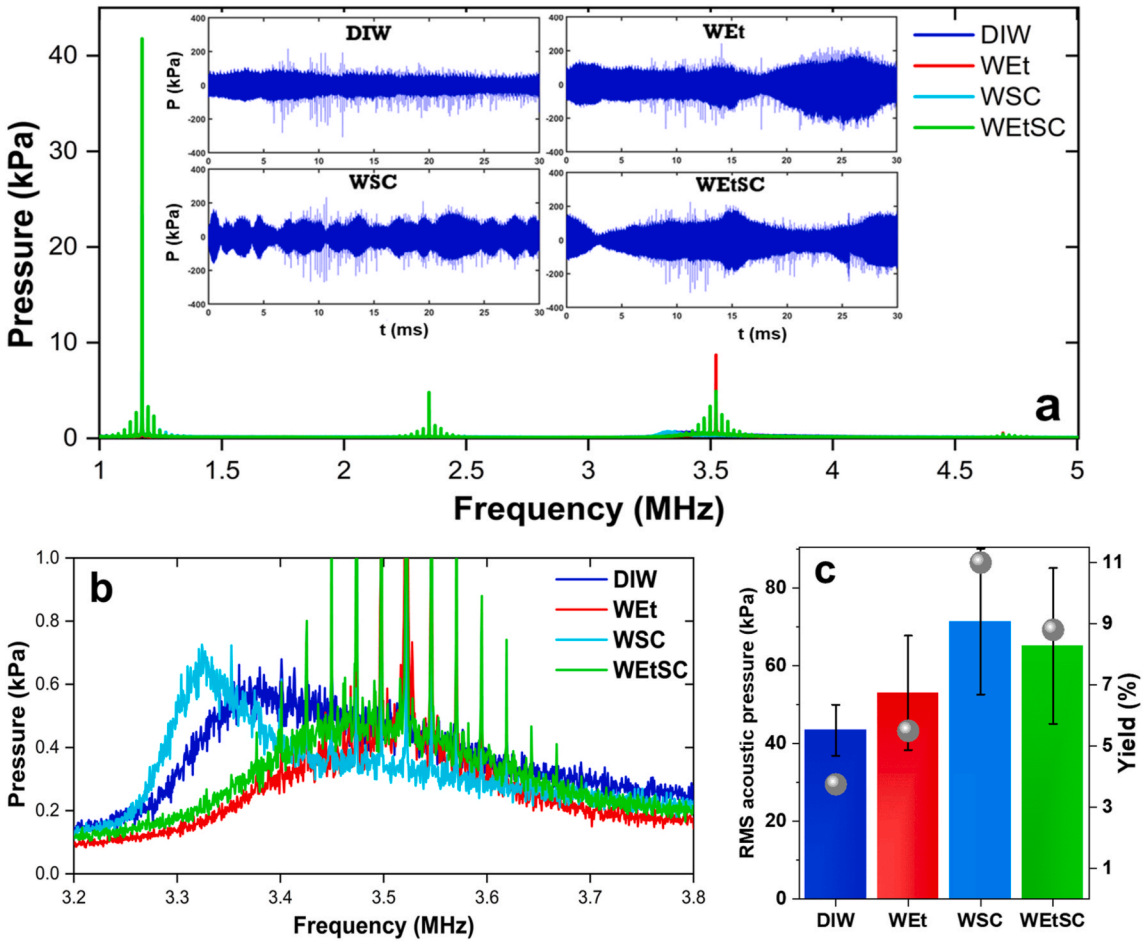

Fig. 4. Examples of spectral acoustic measurements for the ULPE in different solutions (a) and their corresponding waveforms for the general cavitation noise intensity (insets). Spectra were obtained using a fibre-optic sensor sensitive only to MHz-part of the spectra in a wide range from 1 to 5 MHz; (b) Zoomed in spectra from (a) in a smaller range around 3.5 MHz to highlight the area of SWs signals. Based on the spectral data in (a), the RMS acoustic pressures were estimated and plotted with error bars in (c) along with the measured yield (grey spheres, right axis). Note the different Y-axis scales for (a) and (b), the top parts of some peaks in (b) were truncated to emphasize the shape of the main SWs peak. (A colour version of this figure can be viewed online.)

smallest area (as in general the more powerful the SWs, the more chances to break/fragment the graphite powder) with the highest number of defects for the produced graphene samples. Results clearly show the effectiveness of understanding the acoustic emissions in controlling cavitation quality of the produced 2D samples.

Hence, overall, it seems that the WEtSC with an extended cavitation zone (Fig. 4a), prominent shockwaves, vigorously oscillating bubbles (green peaks, Fig. 4b) and higher RMS pressure (Fig. 4c) provides the gentle exfoliation that is important for obtaining high quality graphene flakes [14]. The right combination generates the bubbly mist as seen in Ref. [48], that can cushion the aggressiveness of travelling SWs (the governing mechanism of exfoliation [27]) but at the same time promote vigorous vibration of the tiny bubbles [51] that can infiltrate in-between the loose interlayers of graphite [27] or generate shear stresses in the vicinity [52] that can promote gentle exfoliation. We can conclude, based on the above analysis, that the role of the ethanol and surfactants in ULPE efficiency is through their synergetic effects on the cavitation intensity and produced shockwaves.

4.2. Stabilisation role of ethanol

The fact that DIW ULPE process for graphene production suffers from the weak stability of the FLG flakes is well described in literature [21,22]. We have also observed that as-produced suspension with FLG flakes tend to be unstable (Fig. 3), most likely due to the FLG flakes restacking, leading to more than 50% sedimentation in a week and almost 100% in 2 months. In theory, surfactants are expected to prevent restacking by making flakes–medium interaction more attractive than the weak van der Waals forces between FLG sheets [16,45,46,53,54]. In our experiments we have seen that surfactants drastically improve the stability (57% in 3 months) of the FLG suspension compared to those prepared in DIW. Nevertheless, even better stabilisation effect was achieved in co-solvent of DIW and ethanol (71% in 3 months) and in the co-solvent DIW-ethanol-SC (almost 80%) (see Fig. 3a and Table 1). In the case of SC, ethanol additions boosted the stability from 57 to 78%. Given that, ethanol commands a crucial role in stabilisation of the FLG flakes solution in our dual frequency ULPE.

There are a few reports on the ULPE with ethanol solution, but the mechanisms of ethanol on LPE have not been clarified. For example, similar effect of the ethanol was observed previously in the LPE process with NMP [55], where ethanol showed better stability than some other tested solvents, including methanol, dichloromethane and toluene. However, it was reported that the use of ethanol alone actually decreased the stability of the suspension. It was demonstrated [56] that LPE in some low boiling point solvents could produce a high stabilisation effect >75%, but it was not possible with pure ethanol. Another interesting observation was made by Bose et al. [57] where they showed that due to the polarity difference between water and ethanol and non-covalent functionalization, a better dispersibility and stability of exfoliated flakes were reached in the water-ethanol solution.

Several other papers about surfactant assisted LPE of graphite have shown that the exfoliation process efficiency is drastically increased when water–ethanol co-solvents are used instead of pure ethanol [15, 58]. Recently, based on these reports Wang et al. [45] have demonstrated a high-yield LPE for producing graphene in the co-solvents of ethanol and water without any surfactants, but they used an easy-to-peel electrochemically expanded graphite as the graphite source. However, the stabilisation mechanism of ethanol and its relation to cavitation are still unclear, and need further study.

It was suggested that the reason for the observed stabilisation effect of the water–ethanol medium for ULPE FLG flakes is the modified surface tension, which is decreased from unfavourable 67 mN m^{-1} for water down to ~30 mN m^{-1} for a water–ethanol solution (1:1) at 50 °C [59]. This is consistent with previous reports on the important role played by the liquid surface tension value for LPE of graphite [60,61]. Another possible mechanism [15] involves electrostatic repulsion of graphene in the solution, and it is an essential factor for stabilising graphene. Enhancing electrostatic repulsion mitigates restacking of FLG in the liquid. When both organic co-solvent and surfactant were mixed together to provide the stable liquid medium for graphene ULPE process even better stabilisation effect was observed (Table 1). It is worth noting that when Arao et al. (2017) added SC to the water-organic co-solvent FLG dispersion, most of the flakes agglutinated and sedimented in one day. That difference in the results with our experiments highlights the important role of the cavitation process.

Recently in our group [42] it was shown that addition of ethanol to water has a pronounced effect on stability of graphene suspension, although for the Lf ULPE. It was demonstrated through in situ high-speed imaging that the cavitation zone expands drastically with addition of ethanol to water and, moreover, it shows more uniform distribution of the bubbles of even smaller size. In our case, looking at the waveform in the inset of Fig. 4a, we could notice that in the ethanol-related cases it becomes inhomogeneous in shape. We assume that the waveform gets broader and inconsistent due to the cavitation bubbles behaviour. When we do not see sharp prominent SW peaks in Fig. 4b, these fluctuations and enlargements could be due to the bubbles that do not collapse but rather vigorously vibrate, amplifying the cavitation noise. These differences in cavitation spread and behaviour may play role in affecting the surface properties as well as the dimensions and shape of the graphene flakes, improving thereby the stability of the dispersion. As it was mentioned above, ULPE in ethanol-containing solutions produces more vigorous cavitation (Fig. 4a insets), which could promote the balancing between ethanol's and surfactant's effects on the stability as well as on the quality of FLG dispersion.

Based on the above analysis, we suggest that adding the ethanol to the water-surfactant medium not only helps to match the surface tension but also improves electrostatic repulsion of the flakes exfoliated through ULPE.

5. Conclusion

Different combinations of water, ethanol and green surfactants were used to produce FLG flakes in our original dual frequency ULPE set-up to investigate the effect of the medium onto the cavitation mechanism, which controls and affects the exfoliation of graphene. It was shown that different solutions promoted different cavitation patterns, which in turn influenced the final FLG flakes size, thickness, concentration and stability (Table S1). The structural peculiarities of as-obtained FLG flakes were confirmed in complex characterisation by Raman and UV–vis spectroscopies and HRTEM.

The main conclusion of this study is that the mixture of water–ethanol and SC represents a very efficient green medium for dual frequency ULPE configuration with the high-yield (9%) production of high-quality graphene (equal or less than 5Ls; reduced defects and at least 1 μm^2 area) with a very stable solution that retains 78% of flakes in the suspension after 3 months. An even higher yield of 11% could be achieved using the WSC solution for the production of thinner FLG flakes (4Ls in average) but twice smaller in area and with a higher level of defects.

An acoustic characterisation revealed a new dependency between the ultrasound parameters and the characteristics of graphene produced by dual-frequency ULPE. It was shown that the RMS acoustic pressure of the different solutions is proportional to the yield of the exfoliated FLG flakes.

The presence of SC increased the intensity of shock waves emissions identified by the sharper SW peak around 3.35 MHz. As a result, the more powerful shocks fragmented the flakes into smaller but also more defective pieces.

Important results were obtained in regard to the ethanol presence. From the analysis of the acoustic emissions, ethanol decreased the overall cavitation aggressiveness providing gentler treatment of flakes. It also facilitated the enlarging of the cavitation zone, leading to the improved exfoliation efficiency. It is suggested that adding ethanol to water (1:1 mixture) not only changed the solution surface tension, but also enhanced the electrostatic repulsion, sustaining more vigorous cavitation with secondary tiny 'mist' bubbles, which in turn also promoted a gentler FLG exfoliation with a lower level of defects.

A combination of ethanol and SC in the water solution worked even better as it, on the one hand, supported the gentle treatment to open up flakes due to the water/ethanol cavitation mist and, on the other hand, sustained the powerful shockwaves to initiate exfoliation and loosen the bonds as has been reported elsewhere [27]. Also, the effects on surface tension and electrostatic repulsion properties provided better stabilisation of the FLG flakes dispersion in WEtSC ULPE process.

We can conclude that the role of a proper eco-friendly combination of water with ethanol and surfactant is crucial in the dual frequency ULPE process for graphene production.

CRediT authorship contribution statement

Anastasia V. Tyurnina: Conceptualization, Data curation, Methodology, Formal analysis, Investigation, Validation, Visualization, Writing – original draft. **Justin A. Morton:** Investigation, Data curation, Methodology, Visualization, Writing – review & editing. **Amanpreet Kaur:** Investigation, Data curation, Visualization, Writing – review & editing. **Jiawei Mi:** Funding acquisition. **Nicole Grobert:** Funding acquisition. **Kyriakos Porfyrakis:** Funding acquisition. **Iakovos Tzanakis:** Conceptualization, Funding acquisition, Methodology, Resources, Writing – review & editing. **Dmitry G. Eskin:** Conceptualization, Methodology, Funding acquisition, Project administration, Resources, Supervision, Writing – review & editing.

Declaration of competing interest

The authors declare the following financial interests/personal relationships which may be considered as potential competing interests: Dmitry Eskin reports financial support was provided by UK Engineering and Physical Sciences Research Council (EPSRC).

Acknowledgments

This study is a part of the project "Sustainable and industrially scalable ultrasonic liquid phase exfoliation technologies for manufacturing 2D advanced functional materials" (EcoUltra2D) funded by the UK Engineering and Physical Sciences Research Council (EPSRC) under the grant nos. EP/R031665/1; EP/R031401/1; EP/R031819/1; EP/R031975/1.

Appendix A. Supplementary data

Supplementary data to this article can be found online at https://doi.org/10.1016/j.carbon.2023.01.062.

References

[1] K. Novoselov, A. Geim, S. Morozov, D. Jiang, Y. Zhang, S. Dubonos, I. Grigorieva, A. Firsov, Electric field effect in atomically thin carbon films, Science 306 (5696) (2004) 666–669.

[2] Y. Cao, V. Fatemi, S. Fang, K. Watanabe, T. Taniguchi, E. Kaxiras, P. Jarillo-Herrero, Unconventional superconductivity in magic-angle graphene superlattices, Nature 556 (2018) 43–50.

[3] R. Rudrapati, Graphene: fabrication methods, properties, and applications in modern industries, in: S. Ameen, M. Akhtar, H. Shin (Eds.), Graphene Production and Application, IntechOpen, London, 2020.

[4] M. Sang, J. Shin, K. Kim, K. Yu, Electronic and thermal properties of graphene and recent advances in graphene based electronics applications, Nanomaterials 9 (3) (2019) 374.

[5] Z. Zhang, A. Fraser, S. Ye, G. Merle, J. Barralet, Top-down bottom-up graphene synthesis, Nano Futures 3 (1–32) (2019), 042003.

[6] Y. Bleu, F. Bourquard, T. Tite, A. Loir, C. Maddi, C. Donnet, F. Garrelie, Review of graphene growth from a solid carbon source by pulsed laser deposition (PLD), Front. Chem. 6 (572) (2018) 1–18.

[7] E. Panneflek, Why Investing in Graphene Can Be Lucrative, 9 November 2014 [Online]. Available: https://www.pgmcapital.com/why-investing-in-graphene-can-be-lucrative/.

[8] M. Yi, Z. Shen, Fluid dynamics: an emerging route for the scalable production of graphene in the last five years, RSC Adv. 6 (76) (2016) 72525–72536.

[9] Y. Xu, H. Cao, Y. Xue, Liquid-phase exfoliation of graphene: an overview on exfoliation media, techniques, and challenges, Nanomaterials 8 (942) (2018) 1–32.

[10] P. Karagiannidis, S. Hodge, L. Lombardi, F. Tomarchio, N. Decorde, S. Milana, I. Goykhman, Y. Su, S. Mesite, D. Johnstone, R. Leary, P. Midgley, N. Pugno, F. Torris, A. Ferrari, Microfluidization of graphite and formulation of graphene-based conductive inks, ACS Nano 11 (3) (2017) 2742–2755.

[11] Technical Committee, ISO/TC 229 Nanotechnologies, ISO copyright office, Geneva, 2017, pp. 1–21. https://www.iso.org/standard/64741.html.

[12] K. Paton, E. Varrla, C. Backes, R. Smith, U. Khan, A. O'Neill, C. Boland, M. Lotya, O. Istrate, P. King, T. Higgins, S. Barwich, P. May, P. Puczkarski, I. Ahmed, M. Moebius, H. Pettersson, E. Long, J. Coelho, S. O'Brien, E. M, et al., Scalable production of large quantities of defect-free few-layer graphene by shear exfoliation in liquids, Nat. Mater. 13 (2014) 624–630.

[13] P. Turner, M. Hodnett, R. Doray, J. Carey, Controlled sonication as a route to in-situ graphene flake size control, Sci. Rep. 9 (8) (2019) 8710.

[14] A. Tyurnina, I. Tzanaki, J. Morton, J. Mi, K. Porfyrakis, B. Maciejewska, N. Grobert, D. Eskin, Ultrasonic exfoliation of graphene in water: a key parameter study, Carbon 168 (2020) 737–747.

[15] Y. Arao, F. Mori, M. Kubouchi, Efficient solvent systems for improving production of few- layer graphene in liquid phase exfoliation, Carbon 118 (2017) 18–24.

[16] R. Narayan, S. Kim, Surfactant mediated liquid phase exfoliation of graphene, Nano Converg 2 (2015) 1–19.

[17] S. Gravelle, C. Kamal, L. Botto, Liquid exfoliation of multilayer graphene in sheared solvents: a molecular dynamics investigation, J. Chem. Phys. 152 (8) (2020), 104701.

[18] L. Li, M. Zhou, L. Jin, Y. Mo, E. Xu, H. Chen, L. Liu, M. Wang, X. Chen, H. Zhu, Green preparation of aqueous graphene dispersion and study on its dispersion stability, Materials 13 (12) (2020) 4069, 8.

[19] J. Fernandes, S. Nemala, G.D. Bellis, A. Capasso, Green solvents for the liquid phase exfoliation production of graphene: the promising case of cyrene, Front. Chem. 10 (2022) 1–8.

[20] J. Colemann, Liquid-phase exfoliation of nanotubes and graphene, Adv. Funct. Mater. 19 (2009) 3680–3695.

[21] J. Coleman, Liquid exfoliation of defect-free graphene, Acc. Chem. Res. 46 (1) (2013) 14–22.

[22] K. Ricardo, A. Sendeckia, H. Liu, Surfactant-free exfoliation of graphite in aqueous solutions, Chem. Commun. 50 (2014) 2751–2754.

[23] L. Belyaeva, P. Deursen, K. Barbetsea, G. Schneider, Hydrophilicity of graphene in water through transparency to polar and dispersive interactions, Adv. Mater. 30 (7) (2018), 1703274.

[24] S. Gravelle, C. Kamal, L. Botto, Liquid exfoliation of multilayer graphene in sheared solvents: a molecular dynamics investigation, J. Chem. Phys. 152 (2020) 1–8.

[25] M. Yi, Z. Shen, S. Liang, L. Liu, X. Zhang, S. Ma, Water can stably disperse liquid-exfoliated graphene, Chem. Commun. 49 (2013) 11059–11061.

[26] A. Tyurnina, J. Morton, T. Subroto, M. Khavari, B. Maciejewska, J. Mi, N. Grobert, K. Porfyrakis, I. Tzanaki, D. Eskin, Environment friendly dual-frequency ultrasonic exfoliation of few-layer graphene, Carbon 185 (2021) 536–545.

[27] J. Morton, M. Khavari, L. Qin, B. Maciejewska, I. Tzanakis, A. Tyurnina, N. Grobert, D. Eskin, J. Mi, K. Porfyrakis, P. Prentice, New Insights into sono-exfoliation mechanisms of graphite: in situ high-speed imaging studies and acoustic measurements, Mater. Today 49 (2021) 10–22.

[28] M. Lotya, Y. Hernandez, P. King, R. Smith, V. Nicolosi, L. Karlsson, F. Blighe, S. De, Z. Wang, I. McGovern, G. Duesberg, J. Coleman, Liquid phase production of graphene by exfoliation of graphite in surfactant/water solutions, J. Am. Chem. Soc. 131 (2009) 3611–3620.

[29] A. Green, M. Hersam, Solution phase production of graphene, Nano Lett. 9 (2009) 4031–4036.

[30] K. Nawaz, M. Ayub, M. Khan, A. Hussain, A. Malik, M.N.e. al, Effect of concentration of surfactant on the exfoliation of graphite to graphene in aqueous media, Nanomater. Nanotechnol. 6 (2016) 1–7.

[31] Z. Sun, X. Huang, F. Liu, X. Yang, C. Roesler, R. Fischer, M. Muhler, W. Schuhmann, Amine-based solvents for exfoliating graphite to graphene outperform the dispersing capacity of N-methyl-pyrrolidone and surfactants, Chem. Commun. 50 (2014) 10382–10385.

[32] A. Capasso, A.D.R. Castillo, H. Sun, A. Ansaldo, V. Pellegrini, F. Bonaccorso, Ink-jet printing of graphene for flexible electronics: an environmentally-friendly approach, Solid State Commun. 224 (2015) 53–63.

[33] V. Kravets, A. Grigorenko, R. Nair, P. Blake, S. Anissimova, K. Novoselov, A. Geim, Spectroscopic ellipsometry of graphene and an exciton-shifted van Hove peak in absorption, Phys. Rev. B 81 (15) (2010), 155413.

[34] S. Z, X. L, M. Z, S. H, Q. Lai, Ultraviolet-visible spectroscopy of graphene oxides, AIP Adv. 2 (5) (2012), 032146.

[35] M. Khavari, A. Priyadarshi, A. Hurrell, K. Pericleous, D. Eskin, I. Tzanakis, Characterization of shock waves in power ultrasound, J. Fluid Mech. 186 (2021).

[36] M. Pimenta, M. Dresselhaus, G. Dresselhaus, L. Cancado, A. Jorio, R. Saito, Studying disorder in graphite-based systems by Raman spectroscopy, Phys. Chem. Chem. Phys. 9 (2007) 1276–1290.

[37] M. Dresselhaus, A. Jorio, A. Filho, R. Saito, Defect characterization in graphene and carbon nanotubes using Raman spectroscopy, Phil. Trans. R. Soc. A 368 (2010) 5355–5377, 1932.

[38] A. Eckmann, A. Felten, A. Mishchenko, L. Britnell, R. Krupke, K. Novoselov, C. Casiraghi, Probing the nature of defects in graphene by Raman spectroscopy, Nano Lett. 12 (8) (2012) 3920–3930.

[39] C. Backes, K. Paton, D. Hanlon, S. Yuan, M. Katsnelson, J. Houston, R. Smith, D. McCloskey, J. Donegana, J. Coleman, Spectroscopic metrics allow in-situ measurement of mean size and thickness of liquid-exfoliated few-layer graphene nanosheets, Nanoscale 8 (7) (2016) 4311–4323.

[40] P. Lespade, A. Marchand, M. Couzi, F. Cruege, Caracterisation de materiaux carbones par microspectrometrie Raman, Carbon 22 (4–5) (1984) 375–385.

[41] J.A. Garlow, L.K. Barrett, L. Wu, K. Kisslinger, Y. Zhu, J.F. Pulecio, Large-area growth of turbostratic graphene on Ni(111) via physical vapor deposition, Sci. Rep. 6 (11) (2016), 19804.

[42] J. Morton, A. Kaur, M. Khavari, A. Tyurnina, J. Moffat, A. Priyadarshi, D. Eskin, J. Mi, K. Porfyrakis, P. Prentice, I. Tzanakis, An eco-friendly solution for liquid phase exfoliation of graphite under optimised ultrasonication conditions, Carbon 204 (2023) 434–446.

[43] S. Ray, M. Takafuji, H. Ihara, Peptide-based surface modified silica particles: adsorption materials for dye-loaded wastewater treatment, RSC Adv. 3 (2013) 23664–23672.

[44] U. Khan, H. Porwal, A. O'Neill, K. Nawaz, P. May, J. Coleman, Solvent-exfoliated graphene at extremely high concentration, Langmuir 27 (15) (2011) 9077–9082.

[45] T. Wang, M. Quinn, S. Notley, Enhanced electrical, mechanical and thermal properties by exfoliating graphene platelets of larger lateral dimensions, Carbon 129 (2018) 191–198.

[46] S. Notley, Highly concentrated aqueous suspensions of graphene through ultrasonic exfoliation with continuous surfactant addition, Langmuir 28 (2012) 14110–14113.

[47] A. Kaur, J. Morton, A. Tyurnina, A. Priyadarshi, A. Holland, J. Mi, K. Porfyrakis, D. Eskin, I. Tzanakis, Temperature as a key parameter for graphene sono-exfoliation in water, Ultrason. Sonochem. 90 (9) (2022), 106187.

[48] M. Khavari, Cavitation-Induced Shock Wave Behaviour in Different Liquids, *Ultrasonics Sonochemistry*, no. Special, 2022.

[49] I. Tzanakis, M. Hodnett, G. Lebon, N. Dezhkunov, D. Eskin, Calibration and performance assessment of an innovative high-temperature cavitometer, Sensor Actuator Phys. 240 (2016) 57–69.

[50] L. Yusuf, M. Symes, P. Prentice, Characterising the cavitation activity generated by an ultrasonic horn at varying tip-vibration amplitudes, Ultrason. Sonochem. 70 (12) (2021), 105273.

[51] I. Tzanakis, G. Lebon, D. Eskin, K. Pericleous, Characterizing the cavitation development and acoustic spectrum in various liquids, Ultrason. Sonochem. 34 (2017) 651–662.

[52] L. Qin, B. Maciejewska, T. Subroto, J. Morton, K. Porfyrakis, I. Tzanakis, D. Eskin, N. Grobert, K. Fezza, J. Mi, Ultrafast synchrotron X-ray imaging and multiphysics modelling of liquid phase fatigue exfoliation of graphite under ultrasound, Carbon 186 (2022) 227–237.

[53] A. Sham, S. Notley, Foam stabilisation using surfactant exfoliated graphene, J. Colloid Interface Sci. 469 (2016) 196–204.

[54] J.S. Freeman, K. Goloviznina, H. Li, M. Saunders, G. Warr, A. Pádua, R. Atkin, Ambient energy dispersion and long-term stabilisation of large graphene sheets from graphite using a surface energy matched ionic liquid, Journal of Ionic Liquids 1 (2021) 1–10.

[55] X. Zhang, A. Coleman, N. Katsonis, W. Browne, Dispersion of graphene in ethanol using a simple solvent exchange, Chem. Commun. (J. Chem. Soc. Sect. D) 46 (2010) 7539–7541.

[56] A. O'Neill, U. Khan, P. Nirmalraj, J. Boland, J. Coleman, Graphene dispersion and exfoliation in low boiling point solvents, |J. Phys. Chem. C 115 (2011) 5422–5428.

[57] S. Bose, T. Kuila, A. Mishra, N. Kim, J. Lee, Preparation of non-covalently functionalized graphene using 9-anthracene carboxylic acid, Nanotechnology 22 (7) (2011), 405603.

[58] Y. Liang, M. Hersam, Highly concentrated graphene solutions via polymer enhanced solvent exfoliation and iterative solvent exchange, J. Am. Chem. Soc. 132 (50) (2010) 17661–17663.

[59] G. Vázquez, E. Alvarez, J. Navaza, Surface tension of alcohol + water from 20 to 50 °C, J. Chem. Eng. Data 40 (1995) 611–614.
[60] U. Halim, C. Zheng, Y. Chen, Z. Lin, S. Jiang, R. Cheng, Y. Huang, X. Duan, A rational design of cosolvent exfoliation of layered materials by directly probing liquid–solid interaction, Nat. Commun. 4 (2013) 42213–42219.
[61] Y. Hernandez, V. Nicolosi, M. Lotya, F. Blighe, Z. Sun, S. De, e. al, High-yield production of graphene by liquid-phase exfoliation of graphite, Nat. Nanotechnol. 3 (2008) 563–568.